Short-Packet Communications in Non-Orthogonal Multiple Access Systems

Xiaofang Sun*†, Shihao Yan†, Nan Yang†, Zhiguo Ding‡, Chao Shen*, and Zhangdui Zhong*§
*State Key Lab of Rail Traffic Control and Safety, Beijing Jiaotong University, Beijing, China
†Research School of Engineering, The Australian National University, Canberra, Australia
‡School of Computing and Communications, Lancaster University, Lancaster, UK
§Beijing Engineering Research Center of High-speed Railway Broadband Mobile Communications
Email: {xiaofangsun, chaoshen, zhdzhong}@bjtu.edu.cn, {shihao.yan, nan.yang}@anu.edu.au, z.ding@lancaster.ac.uk

arXiv:1704.06420v1 [cs.IT] 21 Apr 2017

***Abstract*—This work introduces, for the first time, non-orthogonal multiple access (NOMA) into short-packet communications to achieve low latency in wireless networks. Specifically, we address the optimization of transmission rates and power allocation to maximize the effective throughput of the user with a higher channel gain while guaranteeing the other user achieving a certain level of effective throughput. To demonstrate the benefits of NOMA, we analyze the performance of orthogonal multiple access (OMA) as a benchmark. Our examination shows that NOMA can significantly outperform OMA by achieving a higher effective throughput with the same latency or incurring a lower latency to achieve the same effective throughput targets. Surprisingly, we find that the performance gap between NOMA and OMA becomes more prominent when the effective throughput targets at the two users become closer to each other. This demonstrates that NOMA can significantly reduce the latency in the context of short-packet communications with practical constraints.**

I. Introduction

In the fifth generation (5G) wireless ecosystem, the majority of wireless connections will most likely be originated by autonomous machines and devices [1]. Against this background, machine-type communications (MTC) are emerging to support complementary services to that provided by mobile broadband networks. Specifically, massive MTC and ultra-reliable MTC have been identified as two key application scenarios of 5G wireless networks [2]. In MTC, the requirement on latency (besides the reliability) is stringent (e.g., 4 ms) [1], since low latency is pivotal to ensure real-time functionality in interactive communications of machines. In some industrial automation applications, for example, short packets consisting of approximately 100 bits are desired to be transmitted within 100 μs [3]. The challenge in achieving such a low latency lies in the capability to support short-packet communications.

In short-packet communications, as pointed out by [4], the decoding error probability at a receiver is not negligible since the length of a codeword is finite (i.e., the blocklength is finite). This is different from the Shannon capacity theorem, in which the decoding error probability is negligible as the blocklength approaches infinity. Considering the effect of decoding errors, the channel coding rate in finite blocklength regime was derived in [4]. This pioneering work serves as the foundation in examining the performance of short-packet communications. Triggered by [4], the impact of finite blocklength on different communication systems has been widely studied. For example, the achievable channel coding rate in quasi-static multiple-input multiple-output (MIMO) fading channels was examined in [5]. In [6], the tradeoff between reliability, throughput, and latency in short-packet communications was investigated over Rayleigh fading channels. Furthermore, the information theoretic result in [4] was utilized for packet scheduling of a multi-user scenario, wherein the latency-critical packets are transmitted in orthogonal channels [7].

Recently, non-orthogonal multiple access (NOMA) has attracted increasing research interests since it has been recognized as a promising technique that provides superior spectrum efficiency in 5G wireless networks [8]. NOMA is a multi-user multiplexing scheme that achieves multiple access in the power domain [9]. The benefits of NOMA have been widely examined in various wireless communications, such as broadcast channels [10], [11], full-duplex communications [12], and physical layer security [13], [14]. However, its potential benefits in latency reduction in the context of short-packet communications have never been revealed. Turning the question around, the impact of finite blocklength on the performance of NOMA has never been examined, although this impact has been widely investigated for other communications paradigms, as discussed in the previous paragraph. This leaves an important gap in our understanding on the benefits of NOMA in the context of short-packet communications and the impact of finite blocklength on NOMA, which motivates this work.

In this work, *for the first time* we introduce NOMA into short-packet communications in which the benefits of NOMA in latency reduction are explored. We consider a scenario where a single-antenna base station (BS) serves two single-antenna users in the downlink broadcast channel. Specifically, we determine the optimization of transmission rates and power allocation to maximize the effective throughput of one user subject to the constraint on the effective throughput of the other user. In order to explicitly demonstrate the benefits of NOMA, we analyze the performance of orthogonal multiple access (OMA) in the context of short-packet communications as a benchmark. Our examination indicates that NOMA can significantly outperform OMA by achieving a higher effective throughput at one user (subject to the same constraint on the effective throughput at the other user) with the same latency

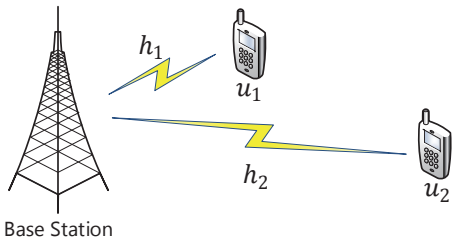

Fig. 1. Illustration of a NOMA system where a single-antenna BS communicates with two single-antenna users.

or incurring a lower latency to achieve the same effective throughput targets. Surprisingly, our results show that the performance gap between NOMA and OMA becomes more prominent when the desired effective throughput targets at the two users become closer to each other.

II. System Model

In this work, we consider a downlink broadcast channel, as depicted in Fig. 1, in which a BS serves two single-antenna users at the same frequency within a finite blocklength. As only one antenna is equipped at BS, it serves the two users either over different time slots (OMA) or simultaneously by adopting NOMA. We define the user with a higher channel gain as user 1 (denoted by u_1) and the other one as user 2 (denoted by u_2). The channel coefficients between the BS and u_1 and between the BS and u_2 are denoted by h_1 and h_2, respectively. We assume that h_1 and h_2 are subject to independent quasi-static Rayleigh fading with equal block length and the associated channel gains are perfectly known by BS. Given the channel gain relationship between u_1 and u_2, we have $|h_1| \geq |h_2|$.

A. Achievable Rate with Finite Blocklength

As per Shannon's channel coding theorem, the decoding error probability at the receiver becomes negligible as the blocklength N approaches infinity [15]. Short-packet communications aims to achieve low latency (e.g., short delay), in which the blocklength should be finite and normally of a small value. As pointed out by [4], the decoding error probability at the receiver is nonnegligible when the blocklength N is finite. Thus, we denote R_i as the channel coding rate with finite blocklength N_i for a given decoding error probability ϵ_i at user i ($i = 1, 2$), and express it as [4], [16]

$$R_i = \log_2(1+\gamma_i) - \sqrt{\frac{V_i}{N_i}}\frac{Q^{-1}(\epsilon_i)}{\ln 2}, \tag{1}$$

where γ_i denotes the signal-to-noise ratio (SNR) at u_i, V_i is the channel dispersion given by

$$V_i = 1 - (1+\gamma_i)^{-2}, \tag{2}$$

$Q^{-1}(\cdot)$ is the inverse Q-function. Equivalently, for a given channel coding rate R_i, the decoding error probability at u_i is approximated by

$$\begin{aligned}\epsilon_i &\triangleq \mathcal{G}(\gamma_i, N_i, R_i)\\ &= Q\left(\ln 2\sqrt{\frac{N_i}{V_i}}\left(\log_2(1+\gamma_i) - R_i\right)\right).\end{aligned} \tag{3}$$

In this paper, we adopt the effective throughput as the objective metric to evaluate the system performance with finite blocklength. Mathematically, the effective throughput (bps) at u_i, T_i, is given by

$$T_i = \frac{N_i}{N}R_i(1-\bar{\epsilon}_i), \tag{4}$$

where $\bar{\epsilon}_i$ is the effective decoding error probability at u_i. For fixed N_i, there exists an optimal value of R_i (or equivalently ϵ_i) that maximizes the effective throughput T_i.

B. Optimization Problem

In our system, the BS needs to serve u_1 and u_2 within N symbol periods (i.e., the finite blocklength is N). The ultimate goal of our design is to achieve the maximum effective throughput of u_1, defined as T_1, while guaranteeing some specific requirements on the effective throughput at u_2 subject to a total power constraint. Mathematically, the optimization problem for the BS with NOMA/OMA is formulated as

$$\max_{\Delta} \quad T_1 \tag{5a}$$

$$\text{s.t.} \quad T_2 \geq \overline{T}_2, \tag{5b}$$

$$P_1N_1 + P_2N_2 \leq \overline{P}N, \tag{5c}$$

$$\Psi(N_1, N_2) \leq N, \tag{5d}$$

where $\Delta = \{R_1, R_2, P_1, P_2, N_1, N_2\}$ represents the variable set that needs to be determined at BS, $\overline{T}_2$ is the minimum required effective throughput at u_2, P_1 and P_2 are the allocated transmit powers to u_1 and u_2, respectively, $\overline{P}$ is the average transmit power within one fading block, $\Psi(N_1, N_2) = \max\{N_1, N_2\}$ for NOMA, and $\Psi(N_1, N_2) = N_1 + N_2$ for OMA. As per (5), we need to design the power allocation and time slots allocation at the BS on top of determining the transmission rates for u_1 and u_2, such that T_1 is maximized subject to given constraints.

III. Design of Non-Orthogonal Multiple Access

In this section, we design a new NOMA scheme to solve the optimization problem given in (5). In the designed scheme, superposition coding (SC) is employed in the transmission such that BS is able to transmit to u_1 and u_2 simultaneously at different power levels. This implies the use of $N_1 = N_2 = N$ in the designed scheme.

A. Transmission to User 1

When the BS adopts NOMA to transmit, the received signal at u_1 at each symbol period is given by

$$y_1 = h_1x + n_1 = h_1(\sqrt{P_1}x_1 + \sqrt{P_2}x_2) + n_1, \tag{6}$$

where $x = \sqrt{P_1}x_1 + \sqrt{P_2}x_2$ is the transmitted signal at the BS, x_1 and x_2 represent the information signals to u_1 and u_2, respectively, and $n_1 \sim \mathcal{CN}(0, \sigma_1^2)$ denotes the additive white Gaussian noise (AWGN) at u_1 with zero mean and variance σ_1^2. Since $|h_1| \geq |h_2|$, we consider that successive interference cancelation (SIC) is employed at u_1 to remove the interference caused by x_2. To do this, u_1 first decodes x_2 treating x_1 as the interference. Following (6), the signal-to-noise-plus-interference ratio (SINR) of x_2 at u_1, denoted by γ_2^1, is given by

$$\gamma_2^1 = \frac{P_2 |h_1|^2}{P_1 |h_1|^2 + \sigma_1^2}. \tag{7}$$

Following (3), the decoding error probability of x_2 at u_1 for given R_2, denoted by ϵ_2^1, is approximated by $\epsilon_2^1 = \mathcal{G}(\gamma_2^1, N, R_2)$. Accordingly, the probability that x_2 is correctly decoded and completely canceled at u_1 is $1 - \epsilon_2^1$. These indicate that perfect SIC may not be guaranteed in our system due to the use of finite blocklength, which is different from the case using infinite blocklength and achieving perfect SIC [8].

If perfect SIC cannot be guaranteed (which occurs with the probability ϵ_2^1), u_1 has to decode x_1 directly subject to the interference caused by x_2. Correspondingly, the SINR of x_1, denoted by γ_1', is given by

$$\gamma_1' = \frac{P_1 |h_1|^2}{P_2 |h_1|^2 + \sigma_1^2}. \tag{8}$$

Then, the decoding error probability of x_1 for given R_1, denoted by ϵ_1', is approximated by $\epsilon_1' = \mathcal{G}(\gamma_1', N, R_1)$.

Differently, if perfect SIC can be guaranteed, following (6) the SNR of x_1 at u_1, denoted by γ_1, is given by

$$\gamma_1 = \frac{P_1 |h_1|^2}{\sigma_1^2}. \tag{9}$$

Accordingly, the decoding error probability of x_1 for given R_1, denoted by ϵ_1, is approximated by $\epsilon_1 = \mathcal{G}(\gamma_1, N, R_1)$.

Considering both (8) and (9), we obtain the effective decoding error probability of x_1 at u_1 as

$$\bar{\epsilon}_1 = (1 - \epsilon_2^1)\epsilon_1 + \epsilon_2^1 \epsilon_1'. \tag{10}$$

B. Transmission to User 2

When the BS adopts NOMA, the received signal at u_2 is given by

$$y_2 = h_2 x + n_2 = h_2(\sqrt{P_1}x_1 + \sqrt{P_2}x_2) + n_2, \tag{11}$$

where $n_2 \sim \mathcal{CN}(0, \sigma_2^2)$ denotes the AWGN at u_2 with zero mean and variance σ_2^2.

Due to $|h_1| \geq |h_2|$, SIC is not needed at u_2. As such, u_2 decodes its own signal directly with the interference caused by x_1. The SINR of x_2 at u_2, denoted by γ_2, is given by

$$\gamma_2 = \frac{P_2 |h_2|^2}{P_1 |h_2|^2 + \sigma_2^2}. \tag{12}$$

Accordingly, the decoding error probability of x_2 for given R_2, denoted by ϵ_2, is approximated by $\epsilon_2 = \mathcal{G}(\gamma_2, N, R_2)$. Since there only exists one decoding strategy at u_2, the decoding error probability ϵ_2 is actually the effective decoding error probability at u_2, i.e., $\bar{\epsilon}_2 = \epsilon_2$.

C. Optimization Problem in NOMA

In NOMA transmission, we have $N_1 = N_2 = N$. Therefore, we rewrite the optimization problem given in (5) as

$$\max_{\Delta_n} \quad T_1 = R_1 \left[(1 - \epsilon_1)\left(1 - \epsilon_2^1\right) + (1 - \epsilon_1')\,\epsilon_2^1\right] \tag{13a}$$

$$\text{s.t.} \quad T_2 \geq \overline{T}_2, \tag{13b}$$

$$P_1 + P_2 \leq \overline{P}, \tag{13c}$$

where $\Delta_n = \{R_1, R_2, P_1, P_2\}$ is the variable set that needs to be determined at the BS in NOMA.

In order to solve (13), we first prove that the equality in (13c) is always achieved when T_1 is maximized, in the following lemma.

***Lemma** 1:* The equality in the power constraint (13c), i.e., $P_1 + P_2 = \overline{P}$, is always guaranteed when the effective throughput T_1 is maximized subject to $T_2 \geq \overline{T}_2$.

Proof: Please refer to Appendix A. ■

From the proof of ***Lemma** 1*, we see that $T_2 > \overline{T}_2$ may happen in NOMA. However, in the following we consider $T_2 = \overline{T}_2$ in NOMA to guarantee a reasonable comparison between NOMA and OMA, since OMA maximizes T_1 when $T_2 = \overline{T}_2$ (which will be discussed in the next section). Also, we consider that R_2 is determined through maximizing T_2 only, which again may not be optimal in NOMA since T_1 is also a function of R_2. We note that this consideration may lead to an unfair comparison between NOMA and OMA since the performance of NOMA is not optimized while that of OMA is optimized. Nevertheless, if we show that NOMA outperforms OMA under these considerations, we can make a conclusion that NOMA definitely outperforms OMA.

With these considerations and following ***Lemma** 1*, the power allocation and R_2 in NOMA are determined such that $T_2 = \overline{T}_2$ is guaranteed with R_2 maximizing T_2 for any given P_2 under the constraint $P_1 + P_2 \leq \overline{P}$. As such, the optimal values of P_1, P_2, and R_2, denoted by P_1^*, P_2^*, and R_2^*, respectively, can be determined efficiently as per (12) and ϵ_2, which are independent of R_1. We next determine the optimal value of R_1 that maximizes T_1 subject to the given constraints. To this end, in the following theorem we prove that there always exists a certain value of R_1 that maximizes T_1 and determine this optimal value.

***Theorem** 1:* There always exists a certain coding rate R_1 that maximizes the effective throughput of u_1. This optimal value, denoted by R_1^*, is the unique solution to

$$\begin{aligned}(1 - \epsilon_2^1)&\left(1 - Q\left(\frac{a - R_1^*}{b}\right) - \frac{R_1^*}{b\sqrt{2\pi}} e^{-\frac{(a-R_1^*)^2}{2b^2}}\right) \\ &= -\epsilon_2^1\left(1 - Q\left(\frac{a' - R_1^*}{b'}\right) - \frac{R_1^*}{b'\sqrt{2\pi}} e^{-\frac{(a'-R_1^*)^2}{2b'^2}}\right),\end{aligned} \tag{14}$$

where $a = \log_2(1+\gamma_1)$, $a' = \log_2(1+\gamma_1')$,

$$b = \frac{1}{\ln 2}\sqrt{\frac{1}{N}\left(1-\frac{1}{(1+\gamma_1)^2}\right)},$$

and

$$b' = \frac{1}{\ln 2}\sqrt{\frac{1}{N}\left(1-\frac{1}{(1+\gamma_1')^2}\right)}.$$

Proof: Please refer to Appendix B. ∎

Although R_1^* cannot be derived in closed form, it can be determined efficiently due to the concavity. Substituting the determined P_1^*, P_2^*, R_1^*, and R_2^* into (4), we obtain the maximum T_1 achieved by NOMA, which is denoted by T_1^*.

IV. Design of Orthogonal Multiple Access

In this section, we adopt OMA in the system and solve the optimization problem given in (5). In OMA, the two users are served in orthogonal time slots and thus, $N_1 + N_2 = N$.

A. Transmission to Two Users

When the BS adopts OMA to serve the two users in orthogonal time slots, the received signal at u_i is given by $y_i = \sqrt{P_i}h_i x_i + n_i$. Due to the orthogonal transmissions to u_1 and u_2, there is no interference at u_1 (or u_2) caused by x_2 (or x_1). As such, the SNR at u_i of x_i is given by

$$\gamma_i = \frac{P_i|h_i|^2}{\sigma_i^2}. \tag{15}$$

Accordingly, the decoding error probability of x_i at u_i for given R_i is approximated by ϵ_i given in (3). Furthermore, in OMA the effective decoding error probability $\bar{\epsilon}_i$ is ϵ_i. We note that for given R_i the corresponding decoding error probability ϵ_i is a function of P_i (not both P_1 and P_2) due to orthogonal transmission.

B. Optimization Problem in OMA

In OMA transmission, we have $N_1 + N_2 = N$. As such, the optimization problem given in (5) is rewritten as

$$\max_{\Delta_o} \quad T_1 = \frac{N_1}{N}R_1(1-\epsilon_1) \tag{16a}$$

$$\text{s.t.} \quad T_2 \geq \overline{T}_2, \tag{16b}$$

$$N_1P_1 + N_2P_2 \leq N\overline{P}, \tag{16c}$$

where $\Delta_o = \{R_1, R_2, P_1, P_2, N_1, N_2\}$ is the variable set that needs to be determined at the BS in OMA. We note that the BS has to optimize the time slots allocation on top of optimizing the transmission rates to u_1 and u_2 and the power allocation in OMA.

In order to solve (16), we first clarify that the equalities in (16b) and (16c) are always guaranteed. This is due to the fact that for any given R_1, R_2, N_1, and N_2, the effective throughputs T_1 and T_2 are monotonically increasing functions of P_1 and P_2, respectively. Taking $T_2 = \overline{T}_2$ and $N_1P_1 + N_2P_2 = \overline{P}$ as constraints, we first fix the time slots allocation (i.e., fix N_1 and N_2) and then optimize R_1, R_2, P_1, and P_2 to maximize the effective throughput T_1 subject to the given constraints. To this end, we note that the optimal values of R_2, P_1, and P_2 can be efficiently determined as per ϵ_2 subject to the constraints $T_2 = \overline{T}_2$ and $N_1P_1 + N_2P_2 = \overline{P}$ for any given N_1 and N_2, which are independent of R_1. We next prove that there always exists a certain coding rate R_1 to maximize T_1 and determine this optimal value.

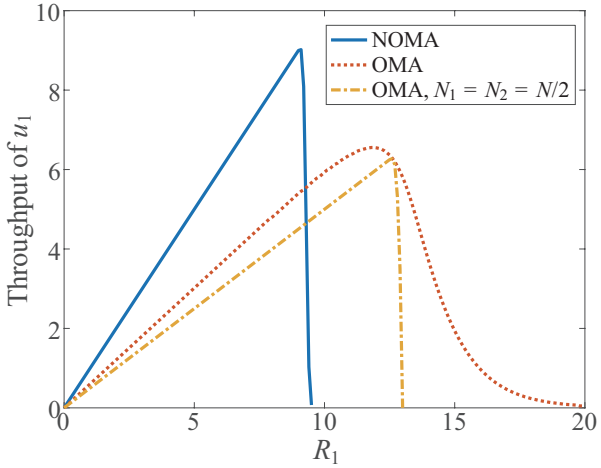

Fig. 2. Effective throughput T_1 achieved by NOMA and OMA versus R_1 with $\overline{T}_2 = 3$, $\overline{\gamma} = 40$ dB, $N = 300$, $|h_1| = 0.8$, and $|h_2| = 0.1$.

***Theorem** 2:* There always exists a certain coding rate R_1 that maximizes T_1. This optimal value, denoted by R_1^*, is the unique solution to

$$Q\left(\frac{c-R_1^*}{d}\right) - \frac{R_1^*}{d\sqrt{2\pi}}e^{-\frac{(c-R_1^*)^2}{2d^2}} = 1, \tag{17}$$

where $c = \log_2(1+\gamma_1)$ and

$$d = \frac{1}{\ln 2}\sqrt{\frac{1}{N_1}\left(1-\frac{1}{(1+\gamma_1)^2}\right)}.$$

Proof: The proof is similar to ***Theorem** 1* given in Appendix B and thus omitted here. ∎

We note that the determined optimal values of P_1, P_2, R_1, and R_2 are functions of N_1 and N_2. Finally, we are able to adopt a one-dimension numerical search method to find the optimal N_1 and N_2, which are used to determine the global optimal P_1, P_2, R_1, and R_2 together with the maximum value of T_1, denoted by T_1^*.

V. Numerical Results

In this section, we present numerical results to evaluate the performance of NOMA with finite blocklength with OMA being the benchmark. Without elsewhere stated, we set the noise power at each user to unit, i.e., $\sigma_1^2 = \sigma_2^2 = 1$, in this section. We also define the average SNR as $\overline{\gamma} = \overline{P}/\sigma_i^2$.

In Fig. 2, we plot the effective throughput of u_1 achieved by NOMA and OMA versus R_1, where the power allocation and R_2 are determined to ensure $T_2 = \overline{T}_2$ subject to $N_1P_1 + N_2P_2 = N\overline{P}$. In this figure, we first observe that there is an optimal value of R_1 that maximizes T_1 in both NOMA and OMA. We also observe that T_1 is concave with respect to R_1 (for

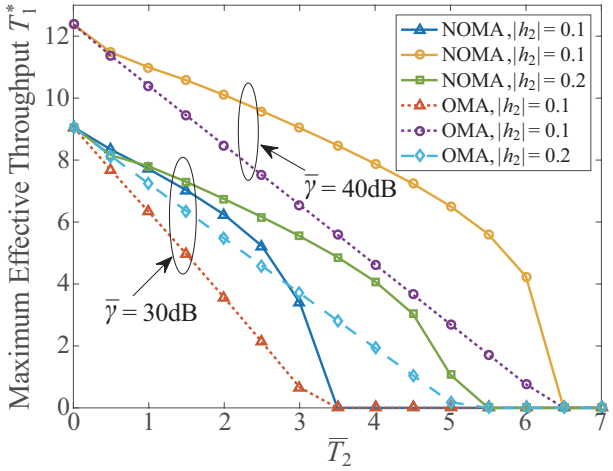

Fig. 3. Maximum effective throughput T_1^* achieved by NOMA and OMA versus $\overline{T}_2$ with $N = 300$ and $|h_1| = 0.8$.

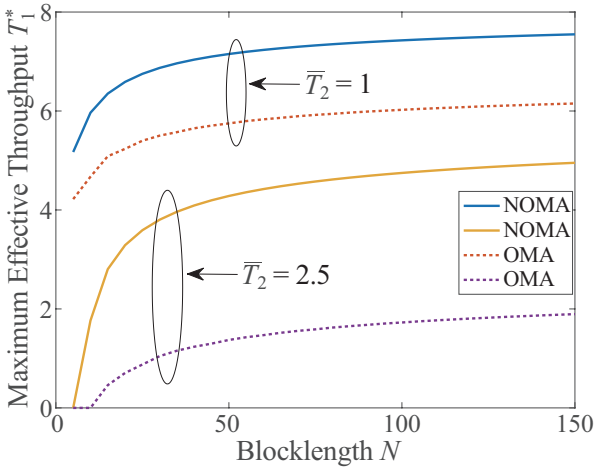

Fig. 4. Maximum effective throughput T_1^* achieved by NOMA and OMA versus blocklength N with $\overline{\gamma} = 30$ dB, $|h_1| = 0.8$, and $|h_2| = 0.1$.

fixed N_1 and N_2 in OMA), which verifies ***Theorems*** *1* and *2*. Furthermore, we observe that for the optimal R_1, NOMA significantly outperforms OMA by achieving a higher T_1, which demonstrates the advantage of NOMA in short-packet communications. This is mainly due to the fact that NOMA serves two users simultaneously and thus reduces the negative impact of the finite blocklength on the throughput. Finally, we observe that NOMA may not outperform OMA if R_1 is predetermined, e.g., $R_1 = 10$. This is due to the interference between the two users in NOMA but not in OMA.

In Fig. 3, we plot the maximum effective throughput of u_1, i.e., T_1^*, versus the constraint on the effective throughput of u_2, i.e., $\overline{T}_2$. First, we observe that T_1^* achieved by NOMA is higher than that achieved by OMA, which is expected. Second, we observe that NOMA and OMA achieve the same maximum effective throughput when $\overline{T}_2 = 0$, since in this case the BS does not have to transmit to u_2 and NOMA becomes OMA. Third, we observe that the gap between T_1^* achieved by NOMA and that achieved by OMA reaches the maximum point in the medium regime of $\overline{T}_2$. This demonstrates that the advantage of NOMA over OMA becomes more prominent when the effective throughput targets at u_1 and u_2 are closer to each other, which applies to most practical scenarios. Fourth, we observe that NOMA and OMA achieve the same maximum effective throughput when $\overline{T}_2$ becomes very large. This is due to the fact that when $\overline{T}_2$ is large, the constraint $T_2 \geq \overline{T}_2$ is hard to guarantee even if all the recourses are allocated to u_2. Fifth, we observe that when $\overline{\gamma}$ becomes higher, T_1^* increases and the performance gap between NOMA and OMA increases. Sixth, we observe that the performance gap increases as the difference between $|h_1|$ and $|h_2|$ increases. In addition, we highlight that in Fig. 3, the power allocation and R_2 are not optimal to NOMA but optimal to OMA, as discussed in Sections III-C and IV-B. Therefore, we conclude that NOMA with optimal power allocation and R_2 definitely achieves a superior performance compared with OMA.

In Fig. 4, we plot the maximum effective throughput T_1^* versus the blocklength N for fixed $\overline{T}_2$. In this figure, we first observe that NOMA outperforms OMA regardless of N. We then observe that the gap between NOMA and OMA initially increases and then keeps constant as N increases. Comparing the value of N for fixed T_1^* (i.e., $T_1^* = 5.97$) in this figure, we observe that the required blocklength of NOMA is significantly less than that of OMA (e.g., $N = 10$ in NOMA while $N = 85$ in OMA when $\overline{T}_2 = 1$). This demonstrates that NOMA can achieve a significantly lower latency than OMA for achieving the same effective throughput. Importantly, this indicates that the NOMA technique enhances the performance of short-packet communications.

VI. Conclusion

This work introduced, for the first time, NOMA in short-packet communications to achieve low latency. With OMA as a benchmark, our analytical and numerical examination demonstrated that NOMA can outperform OMA by achieving a much higher effective throughput at the user with a higher channel gain while ensuring the same effective throughput at the other user. This indicates that NOMA significantly reduces the latency in short-packet communications for achieving the same effective throughput. We further found that the performance gap between NOMA and OMA becomes more prominent as the effective throughputs at the two users become more comparable.

Appendix A
Proof of Lemma 1

We now prove ***Lemma*** *1* by contradiction for any given R_1 and R_2 as follows:

We first assume that the current optimal power allocation $P_1^\dagger$ and $P_2^\dagger$, satisfying $P_1^\dagger + P_2^\dagger < \overline{P}$, can maximize T_1 (denoted by $T_1^\dagger$) and guarantee the constraint $T_2 \geq \overline{T}_2$. We then increase $P_1^\dagger$ and $P_2^\dagger$ by multiplying a common scalar, $\alpha = \overline{P}/(P_1^\dagger + P_2^\dagger)$, to obtain a new power allocation $P_1^\ddagger$ and $P_2^\ddagger$, satisfying $P_1^\ddagger + P_2^\ddagger = \overline{P}$. We note that $P_1^\ddagger > P_1^\dagger$ and $P_1^\dagger > P_1^\ddagger$, due to $\alpha > 1$ caused by $P_1^\dagger + P_2^\dagger < \overline{P}$. Following (7), (8), (9), and (12), we find that

$\gamma_2^1, \gamma_1, \gamma_1'$, and γ_2 increase as $P_1^\dagger$ and $P_2^\dagger$ increase to $P_1^\ddagger$ and $P_2^\ddagger$, respectively. This leads to the fact that the corresponding decoding error probabilities ϵ_1, ϵ_1', ϵ_2^1, and ϵ_2 decrease. We note that T_2 increases as ϵ_2 decreases for a fixed R_2 and thus, the constraint $T_2 \geq \overline{T}_2$ is still guaranteed by $P_1^\ddagger$ and $P_2^\ddagger$.

Following (10) and noting $\epsilon_1 < \epsilon_1'$ due to $\gamma_1 > \gamma_1'$, we find that $\overline{\epsilon}_1$ is a monotonically increasing function of ϵ_1, ϵ_1', and ϵ_2^1, respectively. As such, $\overline{\epsilon}_1$ decreases as $P_1^\dagger$ and $P_2^\dagger$ increase to $P_1^\ddagger$ and $P_2^\ddagger$, respectively. It follows that T_1 increases from $T_1^\dagger$ to $T_1^\ddagger$ (i.e., $T_1^\dagger < T_1^\ddagger$). Notably, this contradicts to the original assumption that $T_1^\dagger$ is the maximum value of T_1 achieved by $P_1^\dagger$ and $P_2^\dagger$. Therefore, we conclude that $P_1 + P_2 = \overline{P}$ is always guaranteed in the optimization problem given in (13).

Appendix B
Proof of Theorem 1

Following (4), we rewrite T_1 as a function of R_1 as

$$\begin{aligned}\mathcal{T}(R_1) =& NR_1\left(1 - Q\left(\frac{a - R_1}{b}\right)\right)(1 - \epsilon_2^1) \\ &+ NR_1\left(1 - Q\left(\frac{a' - R_1}{b'}\right)\right)\epsilon_2^1. \end{aligned} \tag{18}$$

To determine the optimal value of R_1 that maximizes $\mathcal{T}(R_1)$, we next examine the monotonicity and concavity of $\mathcal{T}(R_1)$ with respect to R_1. To this end, we derive the first and second derivatives of $\mathcal{T}(R_1)$ with respect to R_1 as follows:

Based on the differentiation of a definite integral with respect to a parameter [17], the first derivative of $\mathcal{T}(R_1)$ with respect to R_1 is derived as

$$\begin{aligned}\mathcal{T}'(R_1) =& N(1 - \epsilon_2^1)\left(1 - Q\left(\frac{a - R_1}{b}\right) - \frac{R_1\tau}{b}\right) \\ &+ N\epsilon_2^1\left(1 - Q\left(\frac{a' - R_1}{b'}\right) - \frac{R_1\tau'}{b'}\right), \end{aligned} \tag{19}$$

where $\tau = e^{-\frac{(a-R_1)^2}{2b^2}} / \sqrt{2\pi}$ and $\tau' = e^{-\frac{(a'-R_1)^2}{2b'^2}} / \sqrt{2\pi}$.

Similarly, the second derivative of $\mathcal{T}(R_1)$ with respect to R_1 is derived as

$$\begin{aligned}\mathcal{T}''(R_1) =& N(1 - \epsilon_2^1)\left(-\frac{2\tau}{b} - \frac{(a - R_1)R_1\tau}{b^3}\right) \\ &+ N\epsilon_2^1\left(-\frac{2\tau'}{b'} - \frac{(a' - R_1)R_1\tau'}{b'^3}\right). \end{aligned} \tag{20}$$

We note that $a \geq 0$, $a' \geq 0$, $b \geq 0$, and $b' \geq 0$ must hold based on their respective values. Thus, we have $\mathcal{T}'(0) > 0$, due to $0 \leq Q(\frac{a}{b}) \leq 0.5$ and $0 \leq Q(\frac{a'}{b'}) \leq 0.5$, and have $\mathcal{T}''(0) < 0$. When $0 \leq R_1 \leq a'$, following (20) we find that $\mathcal{T}''(R_1)$ keeps negative. Thus, $\mathcal{T}'(R_1)$ keeps decreasing within $0 \leq R_1 \leq a'$.

When $R_1 > a'$, we find that the error probability of u_1 when SIC is not guaranteed is larger than 0.5, i.e., $\epsilon_1' > 0.5$, which leads to zero throughput. As such, the second item in the right-hand side of (18) is negligible when $R_1 > a'$. Due to this, we find that $\mathcal{T}''(R_1)$ still keeps negative and $\mathcal{T}'(R_1)$ keeps decreasing as R_1 increases to a. Furthermore, when R_1 approaches infinity, both $Q(a - R_1)/b)$ and $Q((a' - R_1)/b')$ approach one, whereas both $\frac{R_1}{b\sqrt{2\pi}} \exp\left(-\frac{(a-R_1)^2}{2b^2}\right)$ and $\frac{R_1}{b'\sqrt{2\pi}} \exp\left(-\frac{(a'-R_1)^2}{2b'^2}\right)$ approach zero, as per the L'Hospital's rule. Thus, we obtain $\mathcal{T}'(R_1) \to 0$ as $R_1 \to \infty$.

We next denote the values of R_1 which satisfy $\mathcal{T}'(R_1) = 0$ and $\mathcal{T}''(R_1) = 0$ by $R_1^\dagger$ and $R_1^\ddagger$, respectively. We note that $\mathcal{T}'(R_1)$ decreases from a positive value to $\mathcal{T}'(R_1^\ddagger)$ as R_1 increases from 0 to $R_1^\ddagger$. Since $\mathcal{T}'(R_1)$ is a continuous function and $\mathcal{T}''(R_1)$ keeps positive when $R_1 \geq R_1^\ddagger$, $\mathcal{T}'(R_1)$ increases from $\mathcal{T}'(R_1^\ddagger)$ to 0 as R_1 increases from $R_1^\ddagger$ to infinity, due to $\mathcal{T}'(\infty) \to 0$. This indicates $\mathcal{T}'(R_1^\ddagger) \leq 0$ and $R_1^\dagger \leq R_1^\ddagger$. Therefore, we conclude that when $R_1 \leq R_1^\ddagger$, $\mathcal{T}(R_1)$ is strictly concave with respect to R_1. It follows that the optimal coding rate R_1^* is $R_1^\dagger$, i.e., $R_1^* = R_1^\dagger$, which completes the proof.

References

[1] G. Durisi, T. Koch, and P. Popovski, "Toward massive, ultrareliable, and low-latency wireless communication with short packets," *Proc. IEEE*, vol. 104, no. 9, pp. 1711–1726, Sept. 2016.

[2] "Mobile and wireless communications enablers for the twenty-twenty information society (METIS)," METIS Deliverable D8.4, Apr. 2015.

[3] N. A. Johansson, Y. P. E. Wang, E. Eriksson, and M. Hessler, "Radio access for ultra-reliable and low-latency 5G communications," in *Proc. IEEE ICC Workshops*, London, UK, June 2015, pp. 1184–1189.

[4] Y. Polyanskiy, H. V. Poor, and S. Verdu, "Channel coding rate in the finite blocklength regime," *IEEE Trans. Inf. Theory*, vol. 56, no. 5, pp. 2307–2359, May 2010.

[5] W. Yang, G. Durisi, T. Koch, and Y. Polyanskiy, "Quasi-static multiple-antenna fading channels at finite blocklength," *IEEE Trans. Inf. Theory*, vol. 60, no. 7, pp. 4232–4265, July 2014.

[6] G. Durisi, T. Koch, J. stman, Y. Polyanskiy, and W. Yang, "Short-packet communications over multiple-antenna Rayleigh-fading channels," *IEEE Trans. Commun.*, vol. 64, no. 2, pp. 618–629, Feb. 2016.

[7] S. Xu, T. H. Chang, S. C. Lin, C. Shen, and G. Zhu, "Energy-efficient packet scheduling with finite blocklength codes: Convexity analysis and efficient algorithms," *IEEE Trans. Wireless Commun.*, vol. 15, no. 8, pp. 5527–5540, Aug. 2016.

[8] Z. Ding, Y. Liu, J. Choi, Q. Sun, M. Elkashlan, C. L. I, and H. V. Poor, "Application of non-orthogonal multiple access in LTE and 5G networks," *IEEE Commun. Mag.*, vol. 55, no. 2, pp. 185–191, Feb. 2017.

[9] Y. Saito, Y. Kishiyama, A. Benjebbour, T. Nakamura, A. Li, and K. Higuchi, "Non-orthogonal multiple access (NOMA) for cellular future radio access," in *Proc. IEEE VTC Spring*, Dresden, Germany, June 2013, pp. 1–5.

[10] X. Sun, C. Shen, Y. Xu, S. M. Al-Basit, Z. Ding, N. Yang, and Z. Zhong, "Joint beamforming and power allocation design in downlink non-orthogonal multiple access systems," in *Proc. IEEE Globecom Workshops*, Washington, DC, USA, Dec. 2016, pp. 1–6.

[11] Z. Ding, F. Adachi, and H. V. Poor, "The application of MIMO to non-orthogonal multiple access," *IEEE Trans. Wireless Commun.*, vol. 15, no. 1, pp. 537–552, Jan. 2016.

[12] Y. Sun, D. W. K. Ng, Z. Ding, and R. Schober, "Optimal joint power and subcarrier allocation for full-duplex multicarrier non-orthogonal multiple access systems," *IEEE Trans. Commun.*, vol. 65, no. 3, pp. 1077–1091, Mar. 2017.

[13] Z. Qin, Y. Liu, Z. Ding, Y. Gao, and M. Elkashlan, "Physical layer security for 5G non-orthogonal multiple access in large-scale networks," in *Proc. IEEE ICC*, Kuala Lumpur, Malaysia, May 2016, pp. 1–6.

[14] Y. Liu, Z. Qin, M. Elkashlan, Y. Gao, and L. Hanzo, "Enhancing the physical layer security of non-orthogonal multiple access in large-scale networks," *IEEE Trans. Wireless Commun.*, vol. 16, no. 3, pp. 1656–1672, Mar. 2017.

[15] C. E. Shannon, "A mathematical theory of communication," *The Bell System Technical Journal*, vol. 27, no. 3, pp. 379–423, July 1948.

[16] G. Ozcan and M. C. Gursoy, "Throughput of cognitive radio systems with finite blocklength codes," *IEEE J. Sel. Areas Commun.*, vol. 31, no. 11, pp. 2541–2554, Nov. 2013.

[17] I. Gradshteyn and I. Ryzhik, *Table of Integrals, Series, and Products*. MA,USA: Elsevier Inc, 2007.